REMOTE SENSING · CHANGE DETECTION · ARCGIS PRO

Four Decades of Surface-Water Loss at Lake Mead

A multi-temporal Landsat classification and change-detection analysis, 1981–2022

Analyst	Jared Dumale
Objective	Quantify and visualize change in Lake Mead's surface-water extent over four decades
Data	Seven Landsat scenes (1981–2022), USGS Global Visualization Viewer (GloVis)
Software	ArcGIS Pro — Image Analyst / Classification Tools, Change Detection Wizard
Methods	Supervised K-nearest-neighbor classification, stratified accuracy assessment, raster-to-vector conversion, geometry calculation, post-classification change detection
Headline result	**Classified surface area fell 47.5% (132,631 → 69,692 acres) between 1981 and 2022, with effectively all of the loss occurring after 1999**

Originally produced as a final project for GEOG 883, Penn State MGIS. Revised for portfolio presentation; analysis and figures are unchanged.

Summary

Lake Mead is the largest reservoir in the United States by capacity and the primary water and power source for a large part of the arid Southwest, including Las Vegas, Phoenix, southern California, and northern Mexico. This analysis measured how much of its surface water has disappeared, and when.

Seven Landsat scenes spanning 1981 to 2022 were classified into water and land using supervised classification in ArcGIS Pro, converted to polygons, and measured. Within the study area, classified surface water fell from 132,631 acres in 1981 to 69,692 acres in 2022 — a loss of 62,939 acres, or roughly 98 square miles, representing a 47.5% decline.

The decline is not steady. Between 1981 and 1999 the reservoir showed no net loss at all (+0.9%), including a drop in 1992 that recovered by 1999. Essentially the entire four-decade loss occurs after 1999, at an average of roughly 2,800 acres per year. That inflection is the substantive finding: the reservoir was stable for the first eighteen years of the record and has been in continuous decline for the twenty-three years since.

Problem and Objective

Lake Mead is a linchpin of the economy and habitability of the American Southwest. Dead pool is the elevation at which water can no longer pass through Hoover Dam; if the reservoir reaches it, the consequences for Arizona, California, Nevada, and parts of Mexico would be severe. Public understanding of the trend, however, tends to rest on a handful of widely circulated photographs of the bathtub ring rather than on measured extent.

The objective was to produce an accurate, easily interpreted set of maps and charts showing the extent of surface-water loss at Lake Mead between 1981 and 2022, using measurement rather than illustration. The products are deliberately descriptive rather than predictive: they document what the imagery record shows and make no forecast of future reservoir levels.

Study Area

The study area was drawn to capture the main body of the reservoir while excluding the tributary mouths and confluences where the shoreline is ambiguous and where a small classification error produces a large area error. For this analysis, Lake Mead is defined as the body of water bounded by the Muddy River and Virgin River confluences to the north, Las Vegas Wash to the west, Hoover Dam to the south, and Iceberg Canyon to the east, with the eastern limit following the north–south trajectory of the Arizona–Nevada state line.

This boundary was created as a feature class before any imagery was processed, and every incoming raster was clipped to it. Holding the analysis extent constant across all seven dates is what makes the area values comparable to one another. It also means they are *not* comparable to published surface-area figures for the whole reservoir, which include the Overton Arm and other excluded water.

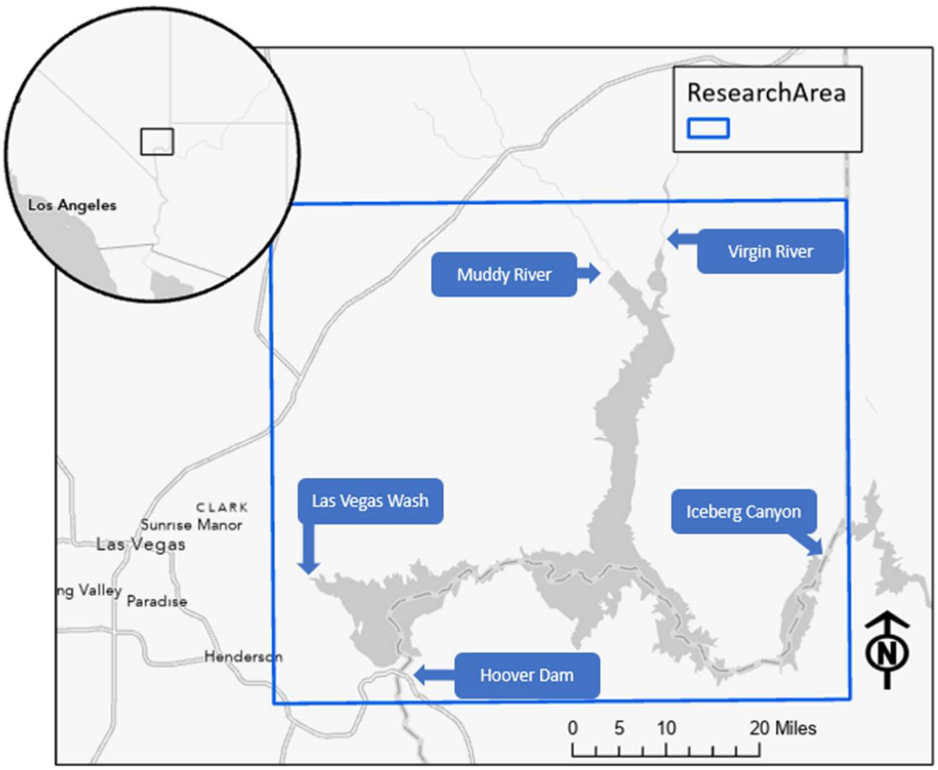

Figure 1. Study area boundary defining Lake Mead for this analysis.

Data

All imagery was obtained from the USGS Global Visualization Viewer (GloVis). Scenes were selected for low cloud cover and acceptable radiometric quality at approximately seven-year intervals across the record.

Year	Platform	Sensor	Resolution	Bands composited
1981	Landsat 2	MSS	79 m native	Green, red, near-infrared
1985–2022	Landsat 5 / 7 / 8	TM / ETM+ / OLI	30 m	Blue, green, red, near-infrared

The 1981 scene is the exception. Landsat 2 carried only the Multispectral Scanner, which has no blue band and a substantially coarser pixel than the Thematic Mapper and the instruments that followed it. The 1981 classification therefore rests on a different and coarser spectral basis than the six later dates, and its shoreline is resolved less precisely. This is carried as a known limitation rather than corrected for; see **Limitations** below.

Method

The same nine-step sequence was applied to each of the seven scenes.

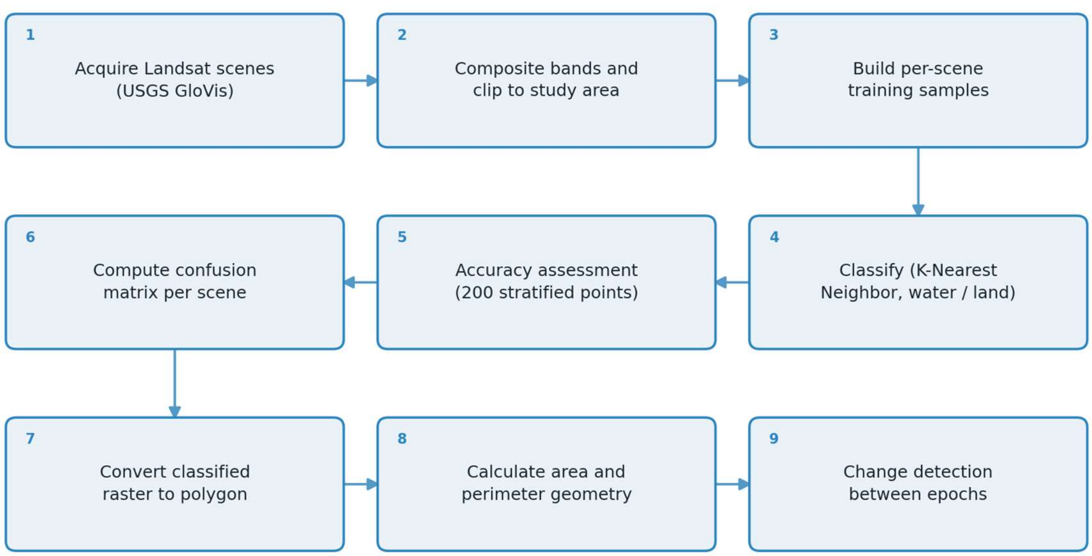

Figure 2. Processing workflow applied to each Landsat scene.

Compositing and clipping

The relevant spectral bands for each scene were combined with the Composite Bands tool and the output extent was clipped to the study area boundary, which keeps processing time and file size manageable and guarantees a constant analysis extent.

Training samples and classification

A two-class schema of water and land was built in the Training Samples Manager and applied to every scene, with a separate saved training sample file for each raster. Samples were built in reverse chronological order, starting with 2022, where the water/land contrast is sharpest, and working backwards; this makes it straightforward to add to the water class and subtract from the land class as the shoreline advances. Classification used the **K-Nearest Neighbor** classifier on a per-pixel basis. No segmentation step was performed, so this is a pixel-based rather than object-based classification.

Each result was checked with the swipe tool against its source raster, with particular attention to the two systematic confusions in this scene type: sediment-laden shallow water misread as land, and cool shadowed canyon walls misread as water. Where either appeared, the training samples were rebuilt and the scene reclassified.

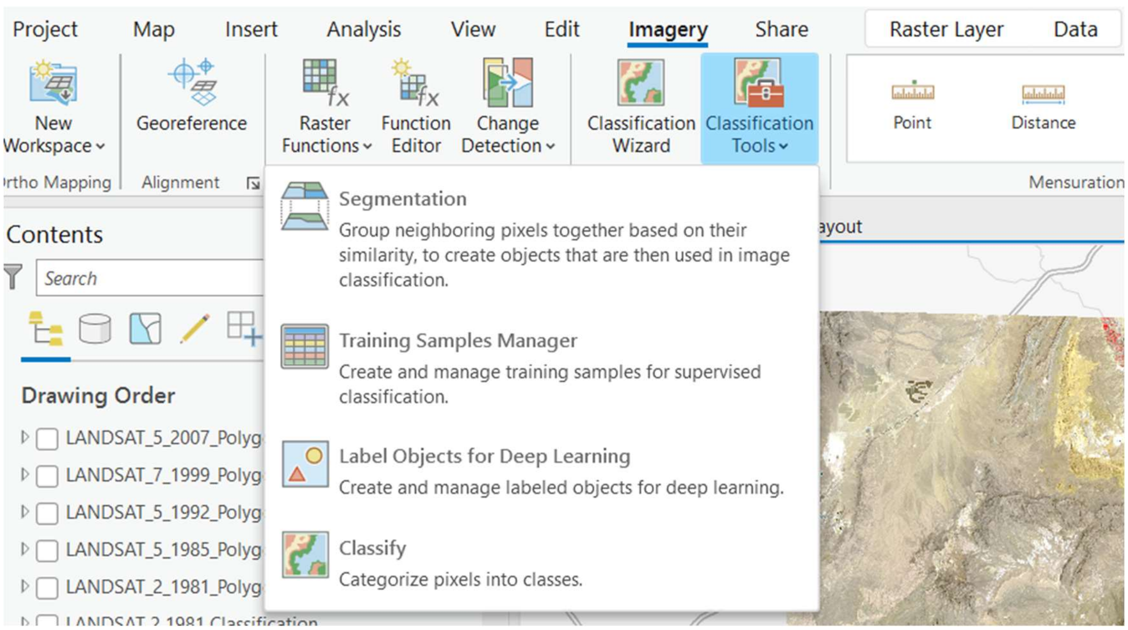

Figure 3. The Classification Tools menu on the ArcGIS Pro Imagery ribbon, containing the Training Samples Manager and Classify tools used in this workflow.

Raster to vector and geometry

Each classified raster was converted with the Raster to Polygon tool. Selecting the single large water polygon at the center of the reservoir isolates the feature of interest, and the swipe tool was used again to confirm the polygon matched the classified extent before exporting it to its own layer. Two double-precision fields, Acreage and Perimeter (km), were added to each polygon layer and populated using Calculate Geometry — area in US survey acres, perimeter length in kilometers. A double field is required here: an integer field would silently truncate the calculated values.

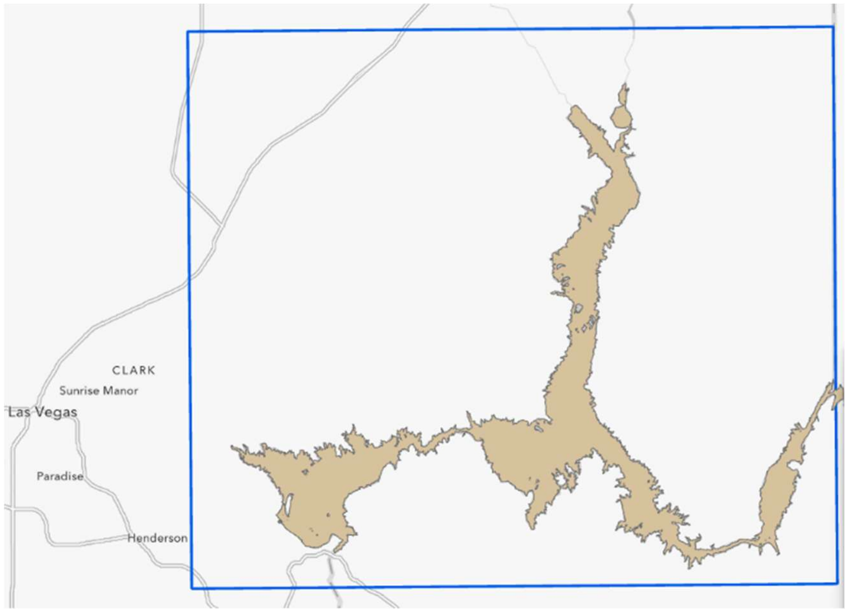

Figure 4. The exported water polygon (brown) derived from the 1999 Landsat 7 classification.

Accuracy Assessment

Each classification was assessed independently. The Create Accuracy Assessment Points tool generated 200 points per scene using the Equalized Stratified Random option, giving 100 points per class. Each point was then interpreted manually against the source Landsat composite for that date and a confusion matrix computed with the Compute Confusion Matrix tool.

Stratifying by class rather than sampling the scene at random matters here. Water occupies a small and shrinking fraction of the study area, so a simple random sample would place most of its points on desert, produce a high overall accuracy, and say almost nothing about the class the analysis depends on. Equalizing the sample forces the assessment onto the water class in every year, including 2022 when water covers the least ground.

Results

Classified surface-water area within the study area declined from 132,631 acres in 1981 to 69,692 acres in 2022, a net loss of 62,939 acres (254.7 km², about 98 square miles) and a 47.5% reduction. Measured from the 1985 peak of 136,634 acres, the loss is 66,942 acres, or 49.0%.

Year	Acres	km²	Change from 1981
1981	132,631	536.7	— (baseline)
1985	136,634	552.9	+3.0%
1992	117,419	475.2	−11.5%
1999	133,818	541.5	+0.9%
2007	95,992	388.5	−27.6%
2013	96,856	392.0	−27.0%
2022	69,692	282.0	**−47.5%**

The shape of the curve matters more than the endpoints. Across the first eighteen years of the record the reservoir shows no net loss: 1985 is above 1981, 1992 falls to 117,419 acres during the early-1990s drought, and 1999 recovers to 133,818 acres, ending the period 0.9% above where it began. From 1999 onward the trend is unbroken and steep: a 47.9% loss over twenty-three years, averaging approximately 2,800 acres per year. The brief flattening between 2007 and 2013 is the only interruption.

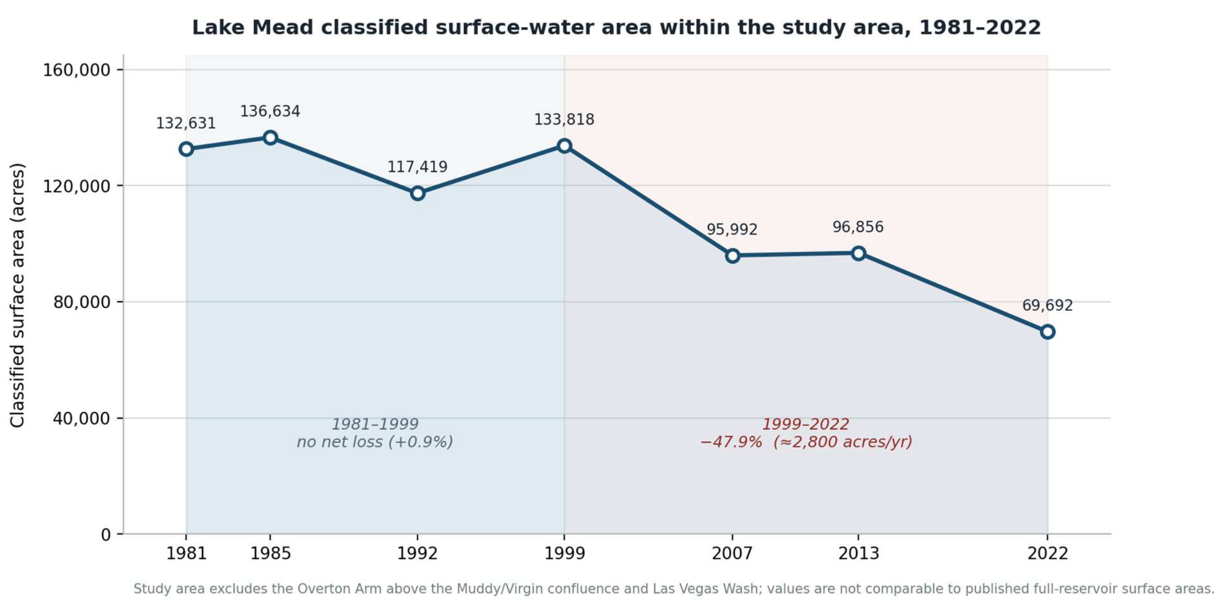

Figure 5. Classified surface-water area by year. The record divides cleanly at 1999: no net change before, sustained decline after.

Mapped against one another, the 1981 and 2022 shorelines show that the loss is not evenly distributed. Retreat is most pronounced in the narrow northern arm and along the shallow margins of the western basins, where gently sloping bathymetry converts a given drop in elevation into a large loss of surface area. The deep central channel narrows but persists.

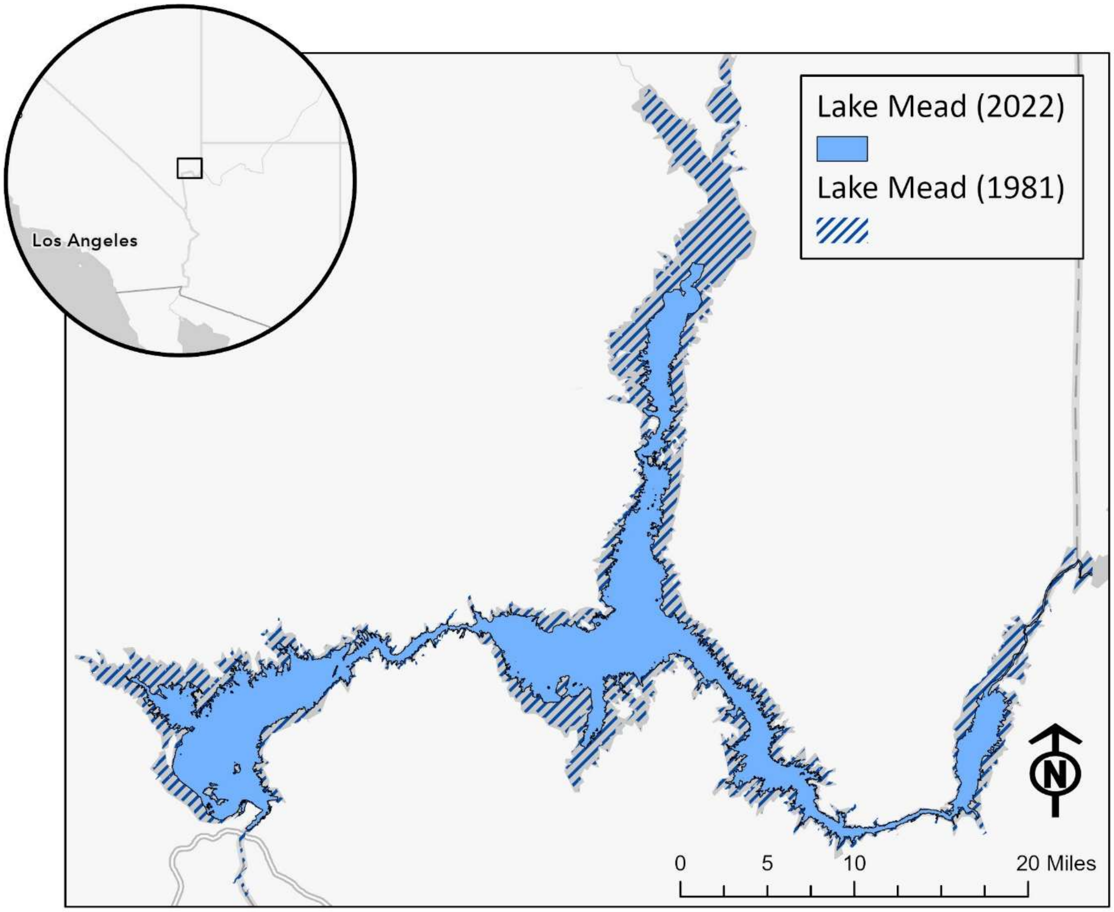

Figure 6. The 2022 shoreline (solid) against the 1981 shoreline (hatched). Hatched area outside the solid fill is surface water lost over the 41-year period.

Post-classification change detection isolates the same pattern by epoch. Between 1981 and 1999 the water-to-land and land-to-water transitions are small and roughly balanced, consistent with the area measurements. Between 1999 and 2022 water-to-land transitions dominate along the entire shoreline.

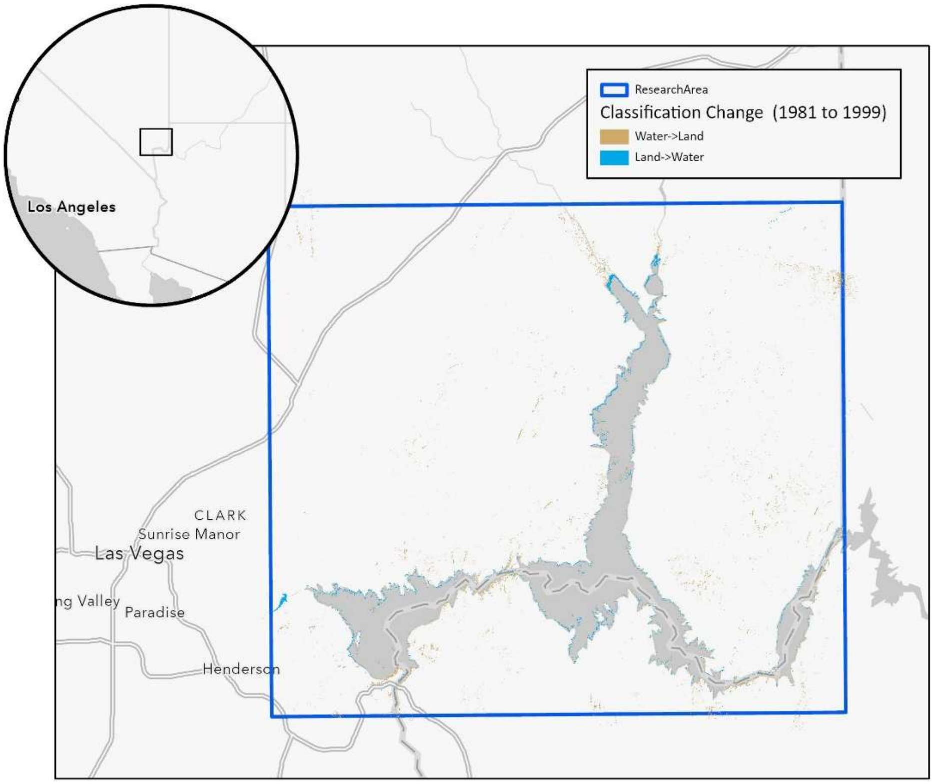

Figure 7. Classification change, 1981–1999. Transitions in both directions are minor; several areas gained water. Scattered pixels away from the shoreline are classification noise rather than real change.

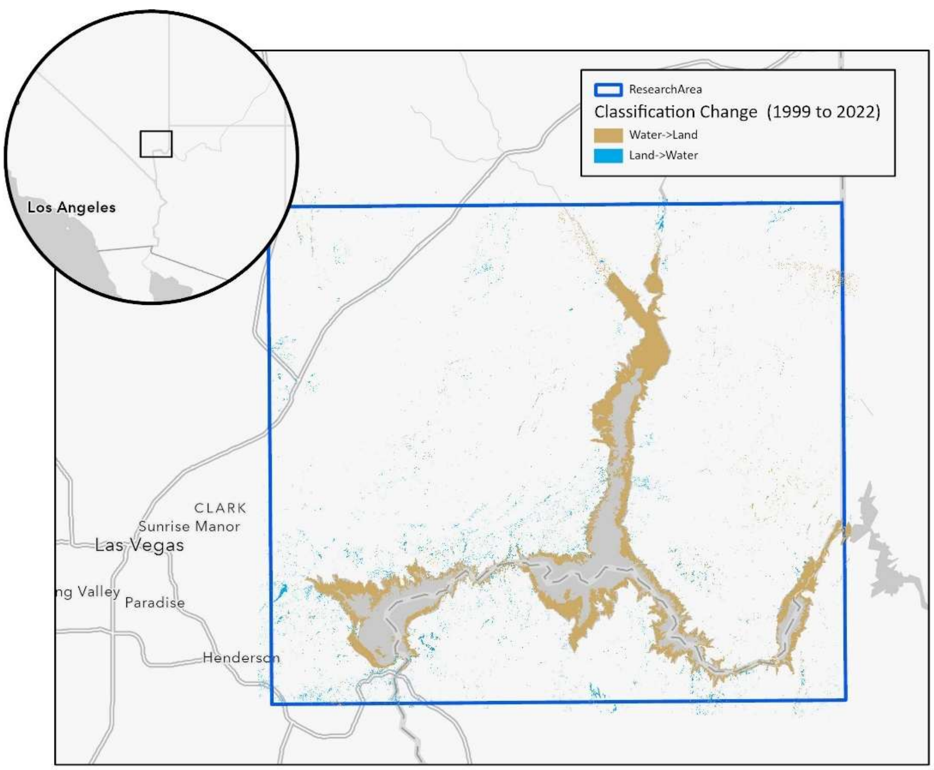

Figure 8. Classification change, 1999–2022. Water-to-land transition (brown) is continuous around the reservoir margin and extensive in the northern arm.

Limitations

Four constraints bound how these results should be read.

- Seasonality is not controlled. Reservoir extent varies within a single year with inflow and drawdown. Unless the seven scenes were selected on or near anniversary dates, some part of the year-to-year difference reflects the month of acquisition rather than the long-term trend. Over a 47.5% change the trend clearly dominates, but the individual year-to-year steps carry this uncertainty.
- The 1981 baseline uses a different sensor. Landsat 2 MSS has coarser pixels and no blue band, so the 1981 shoreline is resolved less precisely than the six later dates and its spectral separation between water and land rests on a different band combination.
- Pixel-based classification produces speckle. The scattered isolated pixels visible away from the shoreline in Figures 7 and 8 are misclassifications, not real change. They have negligible effect on the total area of the main water polygon, which was extracted as a single selected feature, but they are visible in the change-detection products. A majority filter or a segmentation-based approach would suppress them.
- Results are not validated against an independent source. The Bureau of Reclamation publishes a continuous record of Lake Mead elevation and an area–capacity table for the reservoir. Comparing the classified areas against the surface area implied by elevation on each acquisition date would convert this from an internally consistent measurement into an externally validated one. This is the most valuable single extension of the work.

Conclusions

The analysis met its objective: it produced a measured, mapped account of surface-water loss at Lake Mead that can be read at a glance and that rests on documented, repeatable processing rather than on selected photographs.

The substantive finding is the inflection at 1999. A four-decade headline figure of 47.5% loss invites the reading that the reservoir has been draining steadily since the 1980s. It has not. The record shows eighteen years of stability followed by twenty-three years of continuous decline, which points to the late 1990s as the period of interest for anyone asking what changed.

The workflow itself transfers directly. The same sequence applies to any surface-water body with a Landsat record: multi-date acquisition, supervised classification, accuracy assessment, vector conversion, geometry calculation, and post-classification change detection. It extends equally to shoreline, land-cover, and vegetation change.

References

1. Brown, C. B. (1941). Mapping Lake Mead. *Geographical Review, 31*(3), 385–405. https://doi.org/10.2307/210174
2. National Park Service. (2020, September 20). *Overview of Lake Mead*. U.S. Department of the Interior. https://www.nps.gov/lake/learn/nature/overview-of-lake-mead.htm
3. Spicer, S. (2008). When will Lake Mead go dry? *Water Environment & Technology, 20*(5), 41–44. https://www.jstor.org/stable/43890590
4. U.S. Geological Survey. (2005). *Global Visualization Viewer (GloVis)* [Data set]. U.S. Department of the Interior. https://glovis.usgs.gov